EPR studies of the isolated negatively charged silicon vacancies in *n*-type 4*H*- and 6*H*-SiC: Identification of C_{3v} symmetry and silicon sites

N. Mizuochi,[1,2] S. Yamasaki,[2] H. Takizawa,[3] N. Morishita,[3] T. Ohshima,[3] H. Itoh,[3] and J. Isoya[2,4]*

[1]*Institute of Library and Information Science, University of Tsukuba, 1-2 Kasuga, Tsukuba-City, Ibaraki, 305-8550, Japan*
[2]*Diamond Research Center, National Institute of Advanced Industrial Science and Technology (AIST), Tsukuba Central 2, 1-1-1 Umezono, Tsukuba-City, Ibaraki, 305-8568, Japan*
[3]*Japan Atomic Energy Research Institute, 1233 Watanuki, Takasaki-City, Gunma 370-1292, Japan*
[4]*Research Center for Knowledge Communities, University of Tsukuba, 1-2 Kasuga, Tsukuba-City, Ibaraki, 305-8550, Japan*

The isolated negatively charged silicon vacancy (V_{Si}^-) in the hexagonal lattices of 4*H*- and 6*H*-SiC has been studied by electron paramagnetic resonance (EPR). The local structure was suggested to have T_d symmetry from the isotropic *g* value within the resolution of the conventional X-band measurements, from the isotropic ^{29}Si hyperfine interaction of the next-nearest-neighbor silicon atoms and from the absence of the zero-field splitting with the high spin state of $S=3/2$. From the ^{13}C hyperfine spectrum of the nearest-neighbor carbon atoms, the two kinds of V_{Si}^-, denoted V_{Si}^-(I) and V_{Si}^-(II), respectively have been distinguished. V_{Si}^-(I) and V_{Si}^-(II) are assigned to be arising from hexagonal site (*h*) and quasicubic sites (*k* in 4*H*-SiC, k_1 and k_2 in 6*H*-SiC), respectively. In both V_{Si}^-(I) and V_{Si}^-(II), from the ^{13}C hyperfine interactions, the symmetry has been revealed to be C_{3v} with the arrangement of the four nearest-neighbor carbon atoms slightly distorted from a regular tetrahedron.

I. INTRODUCTION

The isolated lattice vacancy is one of the most fundamental intrinsic defects in semiconductor crystals. In the structure determination at the atomic level, for which electron paramagnetic resonance (EPR) is the principal experimental tool, a sufficient concentration of vacancies is produced as radiation damages by irradiation with high energy electrons. The vacancy usually introduces electrical levels into the forbidden gap, and can exist in different charge states. The charge state determined by the number of electrons trapped in the vacancy can be varied by the position of the Fermi level which is controlled by the kind and the concentration of major impurities and by the dose of the electron irradiation.

The important factors which govern the geometric and electronic structures of vacancies are the degree of the lattice structure relaxation attainable and the electron-electron interaction. Thus, even among the isoelectronic vacancies, different symmetries and different spin states emerge in different semiconductor crystals due to the difference in both the strength of the bonding and the degree of the delocalization of the wave function. An interesting example is the negatively charged vacancy (V^-) in silicon ($E_g=1.1$ eV) and in diamond ($E_g=5.5$ eV). In silicon, V^- has C_{2v} symmetry with $S=1/2$.[1] The energy stabilization is achieved by the symmetry-lowering distortion due to Jahn-Teller effect, while the electronic repulsion is lowered by an extensive delocalization. The extent of the wave function along the [110] chain was confirmed by electron nuclear double resonance (ENDOR) measurements.[2] On the other hand, V^- in diamond has T_d symmetry with a high spin ground state ($S=3/2$).[3] The conservation of the T_d symmetry with the high spin ground state of $S=3/2$ is understood from the simple model of defect molecular orbitals, which are linear combi-

nations of the dangling bond orbitals of four atoms around the vacancy. Under the T_d symmetry, the defect molecular orbitals split into an a_1 singlet and a t_2 triplet.[4] With five electrons, the electronic configuration of the ground state is $a_1^2 t_2^3$. With the three unpaired electrons occupying each of three different orbitals of the threefold degenerate t_2 state, the repulsion among the highly localized three electrons is minimized by allowing the electrons to stay far apart. The ground state is the orbitally nondegenerate $^4A_2$ state which is not subject to a Jahn-Teller distortion. The negatively charged silicon vacancy (V_{Si}^-) in 3*C*-SiC (T_d^2, $E_g=2.40$ eV) (Ref. 5) and the neutral Ga vacancy (V_{Ga}^0) in GaP (T_d^2, $E_g=2.26$ eV) (Refs. 6 and 7) were also determined to have T_d symmetry.

For V_{Si}^- in the hexagonal lattices of 4*H*-SiC (C_{6v}^4, $E_g=3.28$ eV) and 6*H*-SiC (C_{6v}^4, $E_g=3.10$ eV), from the EPR spectra which have isotropic *g* values and do not exhibit zero-field splitting (ZFS), the deviation from the regular tetrahedron has not been revealed by the conventional X-band EPR measurements.[8,9] In the T_d symmetry, all three $\Delta M_S=\pm 1$ transitions of $S=3/2$ are superimposed since the ZFS vanishes.[10,11] The effective spin of $S=3/2$ was determined by the ^{29}Si ($I=1/2$, natural abundance 4.68%) ENDOR measurement of the next-nearest-neighbor (NNN) silicon atoms since the ENDOR frequencies $h\nu=|M_S A_{\text{eff}}-g_n\beta_n B|$ depend on the effective spin S.[8] The high spin state was ascribed to an electronic configuration of $a_1^2 t_2^3$ of T_d symmetry. Furthermore, theoretical studies also supported the stability of the high spin state ($S=3/2$) and the T_d symmetry.[8,12]

We have recently demonstrated in the T_{V2a} center in *n*-type 4*H*-SiC (*n*-4*H*-SiC) that the high spin state of $S=3/2$ is also realized in a negatively charged silicon vacancy having C_{3v} symmetry.[13] The EPR spectrum of T_{V2a} does exhibit a fine structure although the ZFS is small ($|D$

$|=35.1$ MHz). Since the central line of the fine structure was hidden underneath the strong signal of V_{Si}^-, the spin multiplicity of $S=3/2$ was determined by the nutation method of the pulsed EPR technique. The measurement of the ^{13}C hyperfine interactions of the nearest-neighbor (NN) carbon atoms identified that the T_{V2a} center is an analog of a single silicon vacancy and revealed that the arrangement of the NN carbon atoms is slightly distorted from a regular tetrahedron. The concentration of the T_{V2a} center is lower by ~ 40 times than that of V_{Si}^- in n-4H-SiC irradiated with 3-MeV electrons at 330 K. The symmetry lowering which is manifested in the ZFS is likely to be caused by a perturbation of the crystal field, presumably by the presence of an accompanying impurity or defect. The triply degenerate t_2 state of an electronic configuration $a_1^2 t_2^3$ under T_d symmetry splits into a_1' and e by the distortion to C_{3v}. The high spin configuration $[a_1'e^2$ or $e^2 a_1']$ which reduces the electron repulsion energy is preferred rather than the low spin configuration expected from the symmetry-lowering crystal field alone. The orbitally nondegenerate $^4A_2$ which is not subject to a Jahn-Teller distortion is derived from the configurations $a_1'e^2$ and $e^2 a_1'$.

A small deviation from an ideal tetrahedron in the atomic arrangements of the SiC$_4$ tetrahedron in 4H- and 6H-SiC was revealed from the high-precision x-ray structure determination.[14,15] The example of the T_{V2a} center indicates that the spin quartet state of V_{Si}^- in the hexagonal polytypes might not necessarily require the T_d symmetry. In our present work, we have measured the angular dependence of the ^{13}C ($I=1/2$, natural abundance 1.1%) hyperfine lines of the four NN atoms of V_{Si}^- in 4H-SiC and in 6H-SiC, since the ^{13}C hyperfine interactions are most crucial in a structural determination of the silicon vacancy. Wimbauer *et al.* reported the^{13}C hyperfine splittings of the NN atoms of V_{Si}^- in 4H-SiC when the magnetic field is parallel to the c axis ([0001] axis).[8] They measured the angular dependence of the ^{13}C hyperfine lines of a NN atom which is located along [0001] (to be denoted the axial carbon atom); however, the angular dependence of the ^{13}C hyperfine lines of the three NN atoms in the basal plane (to be denoted basal carbon atoms) was not reported. We have revealed that the symmetry of V_{Si}^- in both 4H-SiC and 6H-SiC is indeed C_{3v} from the detailed measurements of the ^{13}C hyperfine interaction of the NN atoms.

SiC has many polytypes differing in the stacking sequence of Si-C bilayers. Technologically important polytypes are 3C-, 4H-, and 6H-SiC. In the cubic lattice of 3C-SiC, each silicon and carbon has one site. In performing a detailed local structure determination of defects and impurities in the hexagonal (nH-)SiC crystals, we need to consider that there are $n/2$ inequivalent sites for each silicon and carbon sublattice. In 4H-SiC, each silicon and carbon has two inequivalent sites with either a hexagonal (h) or quasicubic (k) character as shown in Fig. 1(a). In 6H-SiC, each silicon and carbon has one hexagonal (h) site and two quasicubic (k_1 and k_2) sites, as shown in Fig. 1(b). The identification of impurities at the inequivalent lattice sites is important because the properties, such as their energy levels in the band
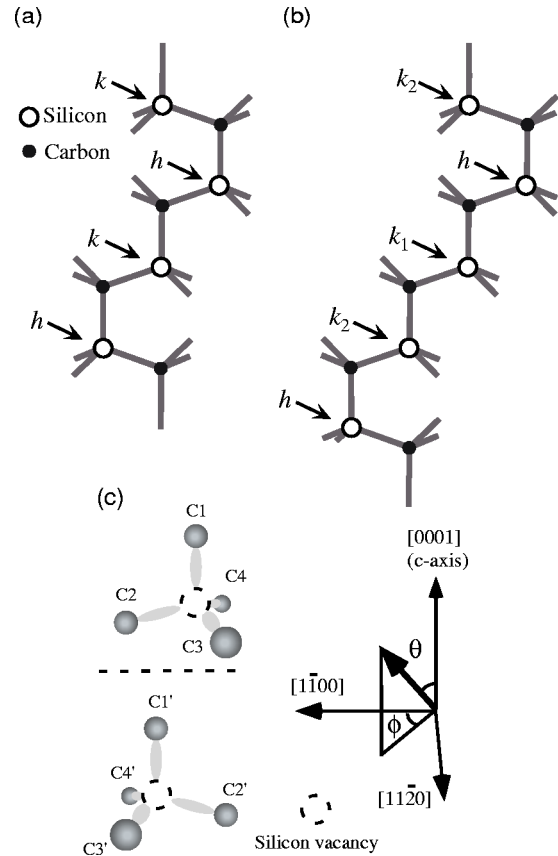

FIG. 1. (a) The crystal structure of 4H-SiC with the positions of the hexagonal (h) site and the quasicubic (k) site for silicon. (b) The crystal structure of 6H-SiC with the positions of the hexagonal (h) site and the two quasicubic (k_1 and k_2) sites for silicon. (c) Two magnetically distinguishable orientations of tetrahedron consisting of NN carbon atoms. The coordinate system used for the principal directions of the spin-Hamiltonian parameters and the magnetic field directions is included. θ is the angle from the [0001] axis. ϕ is the angle from the $[1\bar{1}00]$ axis in the (0001) plane.

gap or the efficiency of doping, usually depend on the site which they occupy. EPR spectra at inequivalent sites in nH-SiC have been distinguished for impurities such as group-III atoms,[9,16–19] group-V atoms,[16,20–23] and transition metal ions.[9,24]

In the hexagonal (nH-)SiC crystals, it is expected that there should be $n/2$ kinds of silicon vacancies corresponding to $n/2$ inequivalent sites of silicon. Recently, two EPR spectra arising from V_{Si}^- in 4H-SiC were resolved at the W band (95 GHz) by the difference in the g value.[25] One with the isotropic g value of $g(k)=2.0032$ was assigned to be V_{Si}^- at the quasicubic site and the other with a slightly anisotropic g value with $g_\parallel(h)=g(k)-0.00004$ and $g_\perp(h)=g(k)-0.00002$ was assigned to be V_{Si}^- at the hexagonal site. In the X band (9.5 GHz) EPR spectra of V_{Si}^- in n-4H-SiC and n-6H-SiC, the primary lines and the ^{29}Si hyperfine lines of NNN atoms are not sufficient to resolve the vacancies at different sites of silicon. In our present work, from the^{13}C hyperfine spectrum of the NN atoms, the two kinds of V_{Si}^-, denoted V_{Si}^-(I) and V_{Si}^-(II), respectively have been distinguished. It will be shown that V_{Si}^-(I) is arising from V_{Si^-} at

the hexagonal site and $V_{Si}^-(\text{II})$ from V_{Si}^- at the quasicubic sites.

II. EXPERIMENT

The samples used in our experiments were single crystalline n-type $4H$- and $6H$-SiC (Nippon Steel: nitrogen dopant) with the carrier concentrations of $\sim 1 \times 10^{17}/\text{cm}^3$. The sample whose thickness is 1.5 mm was cut into the appropriate size (3 mm $\times$ 15 mm) for our EPR measurements in the X band. The crystals of $4H$- and $6H$-SiC were irradiated by 3-MeV electrons with total fluencies of $4 \times 10^{18} e/\text{cm}^2$ and $1 \times 10^{19} e/\text{cm}^2$, respectively. The sample was placed on a water-cooled holder and was kept below 330 K during the electron irradiation. The samples of $4H$-SiC were annealed at 573 K by a muffle furnace so as to decrease the interference with the unidentified signals. The line positions of the continuous wave (cw) EPR spectra were measured at room temperature on a Bruker Elexsys E500 X-band spectrometer by using the amplitude of 100-kHz field modulation of 0.01 mT. The ^{13}C hyperfine lines of V_{Si}^- in $4H$-SiC were measured with the microwave power of 0.2 μW by using the spherical cavity (Bruker ER4122SHQ, $Q_L = 8600$, TE_{011} mode). The ^{13}C hyperfine lines of V_{Si}^- in $6H$-SiC were measured with the microwave power of 2 μW by using the optical transmission cavity (Bruker ER4104OR, $Q_L = 4000$, TE_{102} mode). The calibration of the magnetic field was carried out by measuring simultaneously at room temperature the sample and the perylene cation in conc. H_2SO_4 ($g = 2.002569 \pm 0.000006$) (Refs. 26 and 27) sealed in the capillary which was co-mounted with the sample. In estimating the spin concentration of V_{Si}^-, the signal intensity obtained by double integration of the first derivative signal was compared with that of the EPR signal of Cr^{3+} in a single crystal of ruby[28] comounted with the sample. The relative intensity ratio between the ^{13}C hyperfine line and the primary line was estimated by using the signal intensities obtained by (peak height) $\times (\Delta B_{pp})^2$. In measuring the line width, the modulation amplitude of 0.008 mT was used.

III. RESULTS AND DISCUSSION

A. Angular dependence of ^{13}C hyperfine lines

In conventional X-band EPR measurements of V_{Si}^- of $4H$-SiC and $6H$-SiC, from the primary lines with the isotropic g value and from the absence of the ZFS although with $S = 3/2$, the deviation from an ideal tetrahedron in the arrangement of the four carbon atoms around the silicon vacancy has not been revealed. We have measured the angular dependence of the ^{13}C hyperfine lines of nearest-neighbor carbon atoms in the X-band EPR spectra in a high resolution condition by using small amplitude (0.01 mT) of 100-kHz field modulation.

Here, we describe the features of angular dependence of the ^{13}C hyperfine lines expected for the two cases in which the local arrangement of the four carbon atoms around the silicon vacancy has T_d and C_{3v} symmetries, respectively. As illustrated in Fig. 1, in the two magnetically distinguishable

orientations of a tetrahedron consisting of four carbon atoms around the silicon vacancy, there are altogether eight carbon atoms, two axial carbon atoms labeled C1 and C1$'$, and six basal carbon atoms labeled C2-C4 and C2$'$-C4$'$.

With $\mathbf{B_0} \parallel [0001]$, for both T_d and C_{3v} symmetry, two sets of the ^{13}C hyperfine lines with the intensity ratio 1:3 corresponding to the axial and the basal carbon atoms are expected. For both T_d and C_{3v} symmetries, the ^{13}C hyperfine matrix ($\mathbf{A}^{13}$C) of the axial carbon atoms is uniaxial around $[0001]$, with the maximum hyperfine splitting at $\mathbf{B_0} \parallel [0001]$ and with the minimum at $\mathbf{B_0} \perp [0001]$. Since two axial carbon atoms C1 and C1$'$ are not magnetically distinguishable, the hyperfine line arising from the two axial carbon atoms does not split upon rotation. For both T_d and C_{3v} symmetries, the six basal carbon atoms are symmetry related. In the rotation with $\mathbf{B_0} \perp [1\bar{1}00]$, the ^{13}C hyperfine line of the basal carbon atoms splits into, at most, three lines with the intensity ratio 1:1:1. Upon rotation with $\mathbf{B_0} \perp [11\bar{2}0]$, the ^{13}C hyperfine line of the basal carbon atoms splits into four lines with an intensity ratio 1:2:2:1 at an arbitrary orientation. These patterns of the rotational plots of the line positions of the basal carbon atoms are similar whether the local arrangement of each of two sets of four carbon atoms C1–C4 and C1$'$–C4$'$ is an ideal tetrahedron or a slightly distorted tetrahedron with C_{3v} symmetry. In C_{3v} symmetry, since the axial carbon atoms and the basal carbon atoms are not symmetry related, it is expected that the principal values of $\mathbf{A}^{13}$C should be different between the axial and basal carbon atoms. In the C_{3v} symmetry, the $\mathbf{A}^{13}$C of the basal carbon atoms is nearly uniaxial. The principal axis with the largest principal value is, herein, termed the unique axis. In the C_{3v} symmetry, the unique axis is in a $(11\bar{2}0)$ plane. An orientation which exhibits the maximum hyperfine splitting with the unique axis parallel to $\mathbf{B_0}$ is included in the rotation with $\mathbf{B_0} \perp [11\bar{2}0]$. The minimum hyperfine splitting of the basal carbon atoms occurs either with $\mathbf{B_0}$ perpendicular to the unique axis in a $(11\bar{2}0)$ plane or with $\mathbf{B_0} \parallel [11\bar{2}0]$. In the pattern of the rotational plots of the line positions, it is expected that the C_{3v} symmetry should be revealed by the difference in both the maximum hyperfine splitting and the minimum hyperfine splitting between the axial and the basal carbon atoms. The deviation from an ideal tetrahedron might be also evidenced by the deviation of the angle between the unique axis of $\mathbf{A}^{13}$C of the basal atoms and the c axis $([0001])$ from an ideal tetrahedral angle.

1. 4H-SiC

The EPR spectrum of the electron irradiated n-$4H$-SiC when the magnetic field is parallel to the c axis ($\mathbf{B_0} \parallel [0001]$) is shown in Fig. 2. In the central part of the spectrum, the strong primary line labeled a with the linewidth $\Delta B_{pp} = 0.022$ mT of V_{Si}^- ($g = 2.0028$) (Ref. 13) is observed. The satellite lines labeled b and c arise from ^{29}Si ($I = 1/2$, natural abundance 4.6832%) hyperfine interactions of NNN atoms,[29] the b lines from the configurations with one ^{29}Si nucleus in 12 silicon atoms of the NNN shell, and the c lines from the configurations with two ^{29}Si nuclei in the NNN shell. The hyperfine splitting of 0.298 mT agrees with that was
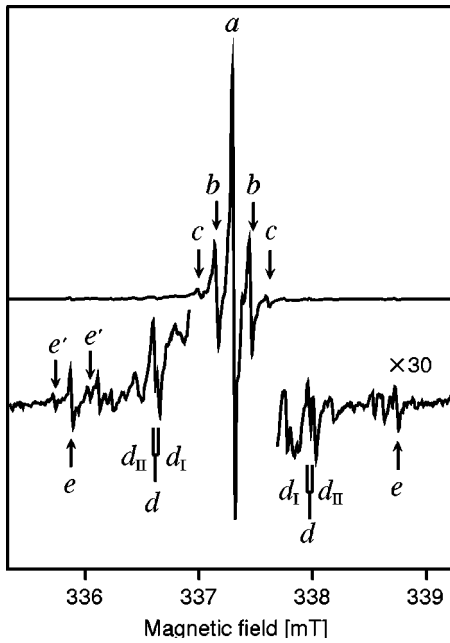
FIG. 2. The EPR spectrum of the electron-irradiated n-type 4H-SiC taken with the magnetic field along the [0001] axis at room temperature. The microwave frequency, the microwave power, and the amplitude of the 100-kHz field modulation were 9.457 GHz, 0.2 μW, and 0.01 mT, respectively. The lower spectrum is the expanded spectrum.

reported.[8] The relative intensity ratios of b/a and c/a, 0.252 and 0.038, respectively, agree with those (0.273 and 0.037, respectively) calculated from the natural abundance of silicon isotopes.[13] The spin concentration of V_{Si}^- was estimated to be 5×10^{17}/cm^3.
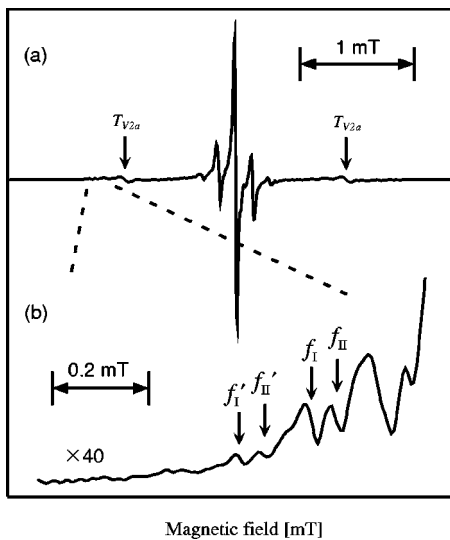

FIG. 3. The EPR spectrum of the electron-irradiated n-type 4H-SiC taken with the magnetic field direction ($\theta=75°$, $\varphi=90°$) at room temperature. The microwave frequency, the microwave power, and the amplitude of the 100-kHz field modulation were 9.457 GHz, 0.2 μW, and 0.01 mT, respectively. The lower spectrum is the expanded spectrum.
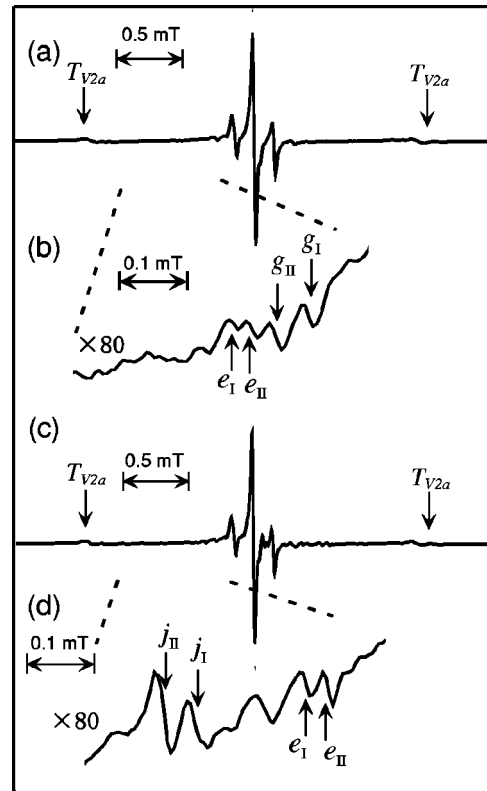

FIG. 4. The EPR spectrum of the electron-irradiated n-type 4H-SiC taken with the magnetic field perpendicular to [0001] at room temperature. (a) The spectrum taken with $\mathbf{B_0} \| [11\bar{2}0]$. (b) The expanded spectrum of (a). (c) The spectrum taken with $\mathbf{B_0} \| [1\bar{1}00]$. (d) The expanded spectrum of (c).

The ^{13}C hyperfine spectrum of the axial and the basal carbon atoms at $\mathbf{B_0} \| [0001]$ was reported by Wimbauer *et al.*[8] In our spectrum shown in Fig. 2, the d and e lines correspond to the ^{13}C hyperfine lines from basal carbon atoms and axial carbon atoms, respectively. In our spectrum taken with a high resolution, we note that the d lines consist of two sets of lines labeled d_I and d_{II}. Thus, we could resolve two kinds of V_{Si}^-, to be denoted V_{Si}^-(I) and V_{Si}^-(II), respectively. At some orientations where the interfering signals did not overlap, it is noticeable that these ^{13}C hyperfine lines accompany weak satellite lines arising from the configurations with one ^{13}C atom in the NN shell and one ^{29}Si atom in the NNN shell, at the line positions of the same hyperfine splitting (0.298 mT) and with the same relative intensity ratio (b/a) as the primary line a. In the spectrum shown in Fig. 2, the satellite lines accompanied with the low field e line are labeled e'.

Upon rotation with $\mathbf{B_0} \perp [1\bar{1}00]$, each of d_I and d_{II} lines at $\mathbf{B_0} \| [0001]$ splits into three lines with the intensity ratio 1:1:1. (labeled f_I, g_I, and h_I for the three lines from d_I, and f_{II}, g_{II}, and h_{II} for the three lines from d_{II}, respectively). In the spectrum with the rotation angle 75° from [0001] shown in Fig. 3, the low field components of the satellite lines (labeled f_I' and f_{II}', respectively) corresponding to b lines of the primary line a are noticed in both f_I and f_{II} lines. This orientation is a typical example that has been used to estimate

FIG. 5. Angular dependence of the line positions of V_{Si}^{-} in $4H$-SiC. The crystal was rotated with the magnetic field in the $(1\bar{1}00)$ plane. In the magnetic field direction $(\theta, \phi=90°)$, $\theta=0°$ for $\mathbf{B_0}\|[0001]$ and $\theta=90°$ for $\mathbf{B_0}\|[11\bar{2}0]$. See the text for the marks representing the line positions observed.
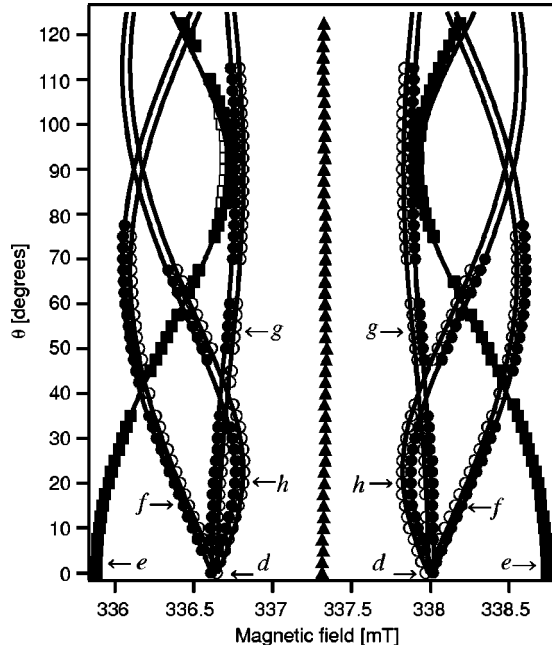

FIG. 6. Angular dependence of the line positions of V_{Si}^{-} in $4H$-SiC. The crystal was rotated with the magnetic field in the $(11\bar{2}0)$ plane. In the magnetic field direction $(\theta, \phi=0°)$, $\theta=0°$ for $\mathbf{B_0}\|[0001]$ and $\theta=90°$ for $\mathbf{B_0}\|[1\bar{1}00]$. See the text for the marks representing the line positions observed.

qthe concentration ratio between V_{Si}^{-}(I) and V_{Si}^{-}(II). In the rotation with $\mathbf{B_0}\perp[11\bar{2}0]$, each of the d_I and d_{II} lines at $\mathbf{B_0}\|[0001]$ splits into four lines with the intensity ratio 1:2:2:1 at an arbitrary angle. The spectrum obtained with $\mathbf{B_0}\|[11\bar{2}0]$ and that with $\mathbf{B_0}\|[1\bar{1}00]$ are shown in Fig. 4. As shown in Fig. 4, a small splitting in the e line was observed at orientations around $\mathbf{B_0}\perp[0001]$, which evidenced that the e line does consist of two lines denoted e_I and e_{II} corresponding to V_{Si}^{-}(I) and V_{Si}^{-}(II), respectively. With $\mathbf{B_0}\|[1\bar{1}00]$, the ^{13}C hyperfine spectrum of the basal carbon atoms in each of V_{Si}^{-}(I) and V_{Si}^{-}(II) has two sets with an intensity ratio 2:4. The sets with the larger intensity are labeled j_I and j_{II}, respectively (Fig. 4), while the other sets with the smaller intensity were interfered with signals from unidentified centers.

The angular dependence of the line positions of ^{13}C hyperfine lines measured upon rotation with $\mathbf{B_0}\perp[1\bar{1}00]$ is shown in Fig. 5. The angular dependence of the line positions of ^{13}C hyperfine lines upon rotation with $\mathbf{B_0}\perp[11\bar{2}0]$ is shown in Fig. 6. In Figs. 5 and 6, each of the points marked with filled triangles (the primary line), open squares [the ^{13}C hyperfine line of axial carbon atoms of V_{Si}^{-}(I)], filled squares [the ^{13}C hyperfine line of axial carbon atoms of V_{Si}^{-}(II)], open circle [the ^{13}C hyperfine line of basal carbon atoms of V_{Si}^{-}(I)], and filled circles [the ^{13}C hyperfine line of basal carbon atoms of V_{Si}^{-}(II)] represents an EPR line position observed in the spectra.

The plots of the line positions upon the rotation with $\mathbf{B_0}\perp[11\bar{2}0]$ shown in Fig. 6 indicate that the maximum hy-
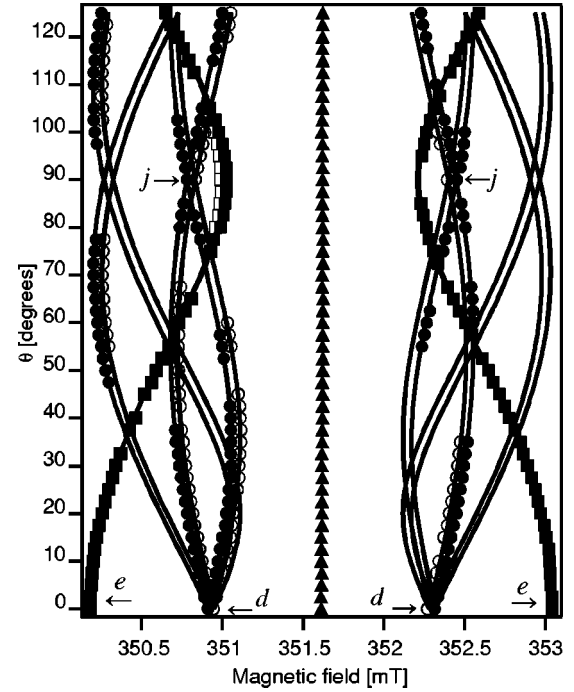
perfine splitting of the basal carbon atoms observed at the unique axis direction is slightly smaller than that of the axial carbon atoms. Furthermore, when $\mathbf{B_0}\|[11\bar{2}0]$ at which the axial carbon atoms labeled e exhibit the minimum hyperfine splitting and the basal carbon atoms labeled g exhibit the minimum one of the rotation with $\mathbf{B_0}\perp[1\bar{1}00]$, their line positions do not superimpose (Fig. 5). Both the number of equivalent carbon atoms at special orientations and the pattern of the roadmap obtained by the angular dependence of the line positions indicate that both V_{Si}^{-}(I) and V_{Si}^{-}(II) do have C_{3v} symmetry.

The signal intensity ratios of the axial (the e line at $\mathbf{B_0}\|[0001]$) and the basal (the d_I and d_{II} lines at $\mathbf{B_0}\|[0001]$) ^{13}C hyperfine lines with respect to the primary line (a) are shown in Table I. The values listed as the observed ratios were obtained as the average among the ratios measured at several orientations where the ^{13}C hyperfine lines were relatively free from the interference of the unidentified signals.

2. 6H-SiC

The EPR spectrum of V_{Si}^{-} in the electron irradiated n-type $6H$-SiC when the magnetic field is parallel to the c axis $(\mathbf{B_0}\|[0001])$ is shown in Fig. 7. The spin concentration of V_{Si}^{-} was estimated to be $1\times10^{18}/cm^3$. In the central part of the spectrum, the strong primary line labeled a (the linewidth $\Delta B_{pp}=0.030$ mT) accompanied with the characteristic satellite lines labeled b and c arising from the ^{29}Si hyperfine interactions of NNN atoms is observed. The g value was determined to be 2.0028 ± 0.0001, that is the same as that of V_{Si}^{-} in $4H$-SiC.

TABLE I. The signal intensity ratio of the ^{13}C hyperfine lines of the NN carbon atoms compared to the primary line.

		Calculated	Observed	comment
4*H*-SiC				
V_{Si}^-	Axial ^{13}C	0.005	0.002	Ref. 8
	Basal ^{13}C	0.015	0.004	
V_{Si}^-(I, II)	Axial ^{13}C	0.005	0.004±0.002	This work
	Basal ^{13}C	0.015	0.012±0.003	
I	Axial ^{13}C		0.002±0.001	
	Basal ^{13}C		0.005±0.002	
II	Axial ^{13}C		0.002±0.001	
	Basal ^{13}C		0.007±0.002	
3*C*-SiC				
V_{Si}^-		0.022	0.018±0.005	Ref. 5
6*H*-SiC				
V_{Si}^-(I, II)	Axial ^{13}C	0.005	0.004±0.002	This work
	Basal ^{13}C	0.015	0.012±0.003	
I	Basal ^{13}C		0.003±0.002	
II	Basal ^{13}C		0.009±0.002	

As for the ^{13}C hyperfine lines of the NN carbon atoms, Schneider *et al.* reported the *c* axis splitting for the axial and the basal carbon atoms.[9] In Fig. 7, the ^{13}C hyperfine lines arising from the axial carbon atoms are labeled *e*. Likewise,
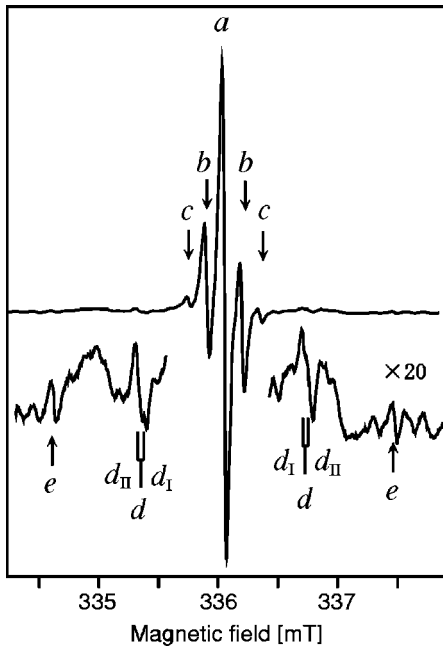

FIG. 7. The EPR spectrum of the electron-irradiated *n*-type 6*H*-SiC taken with the magnetic field along the [0001] axis at room temperature. The microwave frequency, the microwave power, and the amplitude of the 100-kHz field modulation were 9.424 GHz, 2 μW, and 0.01 mT, respectively. The lower spectrum is the expanded spectrum.
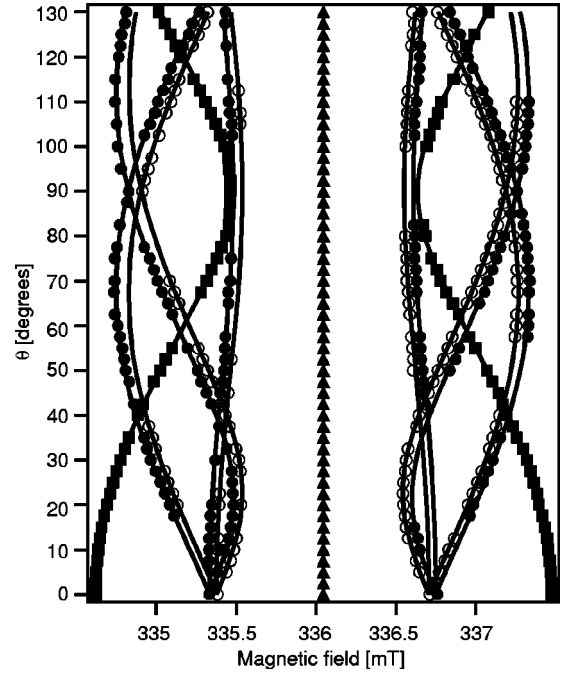

FIG. 8. Angular dependence of the line positions of V_{Si}^- in 6*H*-SiC. The crystal was rotated with the magnetic field in the $(1\bar{1}00)$ plane. In the magnetic field direction $(\theta, \phi=90°)$, $\theta=0°$ for $\mathbf{B_0}\|[0001]$ and $\theta=90°$ for $\mathbf{B_0}\|[11\bar{2}0]$. The filled triangles and the filled squares represent the resonant primary lines and the axial ^{13}C hyperfine lines, respectively. The filled and open circles represent the ^{13}C hyperfine lines of the basal carbon atoms of V_{Si}^-(I) and those of V_{Si}^-(II), respectively.

in 4*H*-SiC, the ^{13}C hyperfine lines arising from the basal carbon atoms are resolved into two sets labeled d_I and d_{II}, respectively. Thus, our high resolution ^{13}C hyperfine spectra taken with the magnetic field modulation of 0.01 mT could distinguish two kinds of V_{Si}^-, to be denoted V_{Si}^-(I) and V_{Si}^-(II), respectively.

The EPR spectra were recorded at 2.5° intervals with the crystal rotated around $[1\bar{1}00]$, with $\mathbf{B_0}\perp[1\bar{1}00]$ at room temperature. The angular dependence of the line positions of the ^{13}C hyperfine lines is shown in Fig. 8. Each point represents the line position observed. In the rotation with $\mathbf{B_0}\perp[1\bar{1}00]$, each of d_I and d_{II} line at $\mathbf{B_0}\|[0001]$ splits into three lines at an arbitrary angle. In the rotation with $\mathbf{B_0}\perp[1\bar{1}00]$, the *e* line could not be resolved into two lines corresponding to V_{Si}^-(I) and V_{Si}^-(II). In obtaining the EPR parameters from the fitting of the line positions, we assumed that the e_I and e_{II} lines superimposed. The signal intensity ratios of the axial and the basal ^{13}C hyperfine lines with respect to the primary line are included in Table I.

B. EPR parameters

The spin Hamiltonian parameters were obtained by fitting observed field strengths and microwave frequencies to the spin Hamiltonian,

$$\mathbf{H_S}=\beta_e\widetilde{\mathbf{S}}\cdot\mathbf{g}\cdot\mathbf{B}+\widetilde{\mathbf{S}}\cdot\mathbf{D}\cdot\mathbf{S}+\widetilde{\mathbf{S}}\cdot\mathbf{A}_{^{13}C}\mathbf{I}-g_{n^{13}C}\beta_n\mathbf{I}\cdot\mathbf{B}, \quad (1)$$

where electron spin $S = 3/2$ and ^{13}C nuclear spin $I = 1/2$. β_e is the Bohr magneton and β_n is the nuclear magneton. The nuclear Zeeman matrix was taken as isotropic ($g_{n^{13}C} = 1.40483$). **g**, **D**, and **A** denote the g matrix, the ZFS tensor, and the hyperfine matrix, respectively. The ZFS matrix **D** was set to zero matrix **O**. The least squares fitting was carried out by using computer program EPR.FOR in which the resonant magnetic fields are calculated by the exact diagonalization of the spin Hamiltonian matrix. The spin Hamiltonian parameters were obtained by using a crystal coordinate system in which the z axis is [0001] and the x axis is [$1\bar{1}00$].

It should be noted that one rotation with **B₀** in the ($1\bar{1}00$) plane or in the ($11\bar{2}0$) plane is sufficient to determine **A**^{13}C of the axial carbon atom C1 when the symmetry of the vacancy belongs to the C_{3v} point group. In the case of the basal carbon atoms, **A**^{13}C of C2 which is one particular carbon atom located on ($11\bar{2}0$) plane can be determined by applying the appropriate symmetry transformations to utilize the line positions of other carbon atoms as the line positions of C2 that should be obtained by the rotation in different planes. Thus, **A**^{13}C of the basal carbon atom C2 can be determined from one rotation with **B₀** in the ($1\bar{1}00$) plane or in the ($11\bar{2}0$) plane. By applying the appropriate symmetry transformations, the parameters belonging to other basal carbon atoms can be obtained. For obtaining **A**^{13}C(C1) and **A**^{13}C(C2) of both V_{Si}^-(I) and V_{Si}^-(II) in 4H-SiC, we used the line positions of both the rotation with **B₀**⊥[$1\bar{1}00$] and that with **B₀**⊥[$11\bar{2}0$]. For obtaining **A**^{13}(C1) and **A**^{13}(C2) of both V_{Si}^-(I) and V_{Si}^-(II) in 6H-SiC, we used the line positions of the rotation with **B₀**⊥[$1\bar{1}00$]. For the least squares fitting, the line positions read from the spectra taken at every 2.5° were used.

The g matrix was obtained from the fitting of the primary lines. In both V_{Si}^-(I) and V_{Si}^-(II) in both 4H-SiC and 6H-SiC, the g matrix was isotropic within a relative accuracy of 0.0001. Recently, the difference in g value between V_{Si}^- at the quasicubic site ($g(k) = 2.0032$, isotropic) and V_{Si}^- at the hexagonal site [$g_\perp(h) - g_\parallel(h) = 0.00002$] in 4$H$-SiC was resolved by the measurement at the W band (95 GHz).[25] The maximum difference in the line positions [$g(k) - g_\parallel(h) = 0.00004$] is estimated to be 0.0066 mT at the X band which is much smaller than the linewidth ($\Delta B_{pp} = 0.022$ mT at **B₀**∥[0001]).

The EPR parameters obtained from the fitting of the line positions of 4H- and 6H-SiC are summarized in Table II. The root-mean-square (rms) error estimates for principal values and principal directions are included. The solid curves in Figs. 5, 6, and 8 are calculated by using the parameters obtained. In Table II, the number of measured line positions used and the rms field deviations (mT) achieved are listed for each fitting of the axial ^{13}C hyperfine lines of V_{Si}^-(I), the basal ^{13}C hyperfine lines of V_{Si}^-(I), the axial ^{13}C hyperfine lines of V_{Si}^-(II), and the basal ^{13}C hyperfine lines of V_{Si}^-(II).

In Table II, the reported values of **A**^{13}C of V_{Si}^- in 4H-SiC (Ref. 8) are included. It should be noted that the averaged

value ($A^{13}C_\parallel = 80.1$ MHz and $A^{13}C_\perp = 34.0$ MHz) of **A**^{13}C(C1) of V_{Si}^-(I) and **A**^{13}C(C1) of V_{Si}^-(II) obtained in this work is in good agreement with the reported values ($A^{13}C_\parallel = 80.1$ MHz and $A^{13}C_\perp = 33.9$ MHz).

C. Structure and silicon sites of V_{Si}^-

The wave function of the unpaired electron is described by a linear combination of atomic orbitals (LCAO) approximation

$$\Psi = \sum_i \eta_i (\alpha_i \varphi_{nsi} + \beta_i \varphi_{npi}), \qquad (2)$$

where the summation is over the surrounding carbon (ns, np: $2s$, $2p$) and silicon (ns, np: $3s$, $3p$) atoms on which the unpaired electrons are delocalized. The fractional unpaired electron population (η_i^2) on the atom concerned and the hybrid ratio (β_i^2/α_i^2, where $\alpha_i^2 + \beta_i^2 = 1$) are estimated from the hyperfine parameters. In the estimation ($\eta_i^2 \alpha_i^2 a_0 = A_{iso}$, $\eta_i^2 \beta_i^2 b_0 = A_{aniso}$), we used $a_0 = 3776.92$ MHz, and $b_0 = 107.39$ MHz for ^{13}C.[30,31] The results are listed in Table III. In the wave function of the unpaired electron of V_{Si}^- of 4H-SiC, the fraction which localizes on the four NN carbon atoms is 63.4% and 63.6% for V_{Si}^-(I) and V_{Si}^-(II), respectively. In the wave function of the unpaired electron of V_{Si}^- of 6H-SiC, the fraction which localizes on the four NN carbon atoms is 63.6% and 65.1% for V_{Si}^-(I) and V_{Si}^-(II), respectively. As for the 12 NNN silicon atoms, the hyperfine splitting observed as the satellite lines of the primary line was isotropic within the resolution of our measurements and the anisotropic part which is arising from the contribution of $3p$ orbital could not be measured. In V_{Si}^- of both 4H-SiC and 6H-SiC, the sum of the contribution of the $3s$ orbital of 12 NNN silicon atoms is estimated to be 2.3% by using $a_0 = -4594.12$ MHz for ^{29}Si.

From the pattern of the rotational plots, it is determined that both V_{Si}^-(I) and V_{Si}^-(II) in both 4H-SiC and 6H-SiC have a C_{3v} symmetry. With a C_{3v} symmetry, the axial carbon atom and basal carbon atom are not symmetry related. The deviation from an ideal tetrahedral symmetry is confirmed by the fact that, as seen from Table II, the principal values of **A**^{13}C(C1) are not the same as the principal values of **A**^{13}C(C2). From the small difference of the principal values of **A**^{13}C between the axial carbon atoms and the basal carbon atoms, it is inferred that the distortion of the structure from T_d to C_{3v} is considered to be very small. The polar angle θ of the unique axis of the ^{13}C hyperfine matrix of basal carbon atoms, 110.0°, 110.0°, 109.2°, and 109.1° for V_{Si}^-(I) in 4H-SiC and in 6H-SiC and V_{Si}^-(II) in 4H-SiC and in 6H-SiC, respectively, is deviated from an ideal tetrahedral angle (109.47°). The ^{13}C hyperfine spectra confirm that the NN atoms are four carbon atoms arranged in a configuration close to regular tetrahedron and that these carbon atoms have a relatively large spin density. We note that the contribution to the wave function of the unpaired electron from the atomic orbital of carbon is almost purely p, as shown in Table III. The dominant structure relaxation in V_{Si}^- is likely to be outward displacements of the NN atoms.

TABLE II. EPR parameters of the negatively charged silicon vacancies in SiC.

Polytype		g	Principal values (MHz)	Principal directions	N^a	rms^b (mT)	Comment
4H-SiC							
	V_{Si}^-	2.0034±0.0001	$A_\parallel$C(C1) = 80.1	[0001] ($\theta = 0°$)			Ref. 8
			$A_\perp$C(C1) = 33.9	Axially symmetric			
	V_{Si}^-(I)	2.0028±0.0001^c	$A_\parallel$C(C1) = 80.2±0.1	[0001] ($\theta = 0°$)	175	0.01	This work
			$A_\perp$C(C1) = 33.2±0.1	Axially symmetric			
			A_xC(C2) = 76.3±0.1	$\theta = 110.0° ± 0.1°$, $\phi = 0°$	252	0.01	
			A_yC(C2) = 28.3±0.1	$\theta = 90°$, $\phi = 90°$			
			A_zC(C2) = 28.2±0.1	$\theta = 20.0° ± 0.1°$, $\phi = 0°$			
	V_{Si}^-(II)	2.0028±0.0001^c	$A_\parallel$C(C1) = 80.1±0.1	[0001] ($\theta = 0°$)	169	0.01	This work
			$A_\perp$C(C1) = 33.8±0.1	Axially symmetric			
			A_xC(C2) = 79.4±0.1	$\theta = 109.2° ± 0.1°$, $\phi = 0°$	285	0.01	
			A_yC(C2) = 31.4±0.1	$\theta = 90°$, $\phi = 90°$			
			A_zC(C2) = 31.2±0.1	$\theta = 19.2° ± 0.1°$, $\phi = 0°$			
	T_{V2a}	2.0029±0.0001	$A_\parallel$C(C1) = 80.3±0.1	[0001] ($\theta = 0°$)	61	0.01	Ref. 13
			$A_\perp$C(C1) = 34.8±0.2	Axially symmetric			
			A_xC(C2) = 75.8±0.4	$\theta = 107.5° ± 0.3°$, $\phi = 0°$	175	0.03	
			A_yC(C2) = 31.3±0.2	$\theta = 17.5° ± 0.3°$, $\phi = 0°$			
			A_zC(C2) = 27.2±0.6	$\theta = 90°$, $\phi = 90°$			
6H-SiC							
	V_{Si}^-(I)	2.0028±0.0001^c	$A_\parallel$C(C1) = 80.0±0.1	[0001] ($\theta = 0°$)	86	0.01	This work
			$A_\perp$C(C1) = 32.8±0.1	Axially symmetric			
			A_xC(C2) = 75.8±0.1	$\theta = 110.0° ± 0.1°$, $\phi = 0°$	174	0.01	
			A_yC(C2) = 28.4±0.1	$\theta = 90°$, $\phi = 90°$			
			A_zC(C2) = 28.2±0.1	$\theta = 20.0° ± 0.1°$, $\phi = 0°$			
	V_{Si}^-(II)	2.0028±0.0001^c	$A_\parallel$C(C1) = 80.0±0.1	[0001] ($\theta = 0°$)	86	0.01	This work
			$A_\perp$C(C1) = 32.8±0.1	Axially symmetric			
			A_xC(C2) = 80.3±0.1	$\theta = 109.1° ± 0.1°$, $\phi = 0°$	145	0.01	
			A_yC(C2) = 31.6±0.1	$\theta = 90°$, $\phi = 90°$			
			A_zC(C2) = 31.4±0.1	$\theta = 19.1° ± 0.1°$, $\phi = 0°$			
3C-SiC							
	V_{Si}^-	2.0029±0.0001	$A_\parallel$C(C1) = 80.4	[111]			Ref. 5
			$A_\perp$C(C1) = 33.0	Axially symmetric			

^{a}The number of the measured line positions.
^{b}Root-mean-square field deviation.
^{c}In our work, the g value was determined by measuring simultaneously with the reference sample.

While the C_{3v} symmetry is revealed by the ^{13}C hyperfine interactions of the NN atoms, the ZFS has not been observed by conventional, cw EPR technique. By using the nutation method of pulsed EPR technique, the presence of ZFS in V_{Si}^- in 4H-SiC was revealed.[13] We showed that the primary line of V_{Si}^- in 4H-SiC consists of all three $\Delta M_S = \pm 1$ transitions of $S = 3/2$ of non-distorted configuration and $|S, M_S\rangle = |3/2, 1/2\rangle \Leftrightarrow |3/2, -1/2\rangle$ transition of slightly distorted configuration. The nutation frequency of non-distorted configuration of which three $\Delta M_S = \pm 1$ transitions are superimposed or are located within the extent of the excitation bandwidth of the microwave pulse ($B_1 \sim 0.3$ mT) is $\omega_1 = g \beta_e B_1 / \hbar$. The nutation frequency of slightly distorted configuration is $2\omega_1$

since only $|3/2, 1/2\rangle \Leftrightarrow |3/2, -1/2\rangle$ transition is excited by the microwave pulse with the $|3/2, \pm 3/2\rangle \Leftrightarrow |3/2, \pm 1/2\rangle$ transitions being located away from the $|3/2, 1/2\rangle \Leftrightarrow |3/2, -1/2\rangle$ transition by at least $\sim B_1$ due to the ZFS. In slightly distorted configuration, the $|3/2, \pm 3/2\rangle \Leftrightarrow |3/2, \pm 1/2\rangle$ transitions which are likely to be broadened by a distribution of ZFS presumably due to local strains are too broad to be observed as separate signals. Thus, the magnitude of ZFS is distributed from a value smaller than B_1 to one larger than B_1. The criterion of whether configurations are nondistorted or distorted in the nutation experiments depends on the relative magnitude between $|D|$ and B_1.

In 4H-SiC, there are two types of silicon sites, one with

TABLE III. Hyperfine and orbital parameters of V_{Si}^-.

	A_{iso} (MHz)	A_{aniso} (MHz)	η^2	β^2/α^2
4H-SiC				
$\mathbf{A}^{13}$C(C1):I	48.9 ± 0.4	15.7 ± 0.4	0.159	11.3
$\mathbf{A}^{13}$C(C1):II	49.2 ± 0.4	15.7 ± 0.4	0.159	11.2
$\mathbf{A}^{13}$C(C2):I	44.3 ± 0.4	16.0 ± 0.4	0.161	12.7
$\mathbf{A}^{13}$C(C2):II	47.3 ± 0.4	16.0 ± 0.4	0.162	11.9
6H-SiC				
$\mathbf{A}^{13}$C(C1)	48.5 ± 0.2	15.7 ± 0.2	0.159	11.4
$\mathbf{A}^{13}$C(C2):I	44.2 ± 0.2	15.8 ± 0.2	0.159	12.6
$\mathbf{A}^{13}$C(C2):II	47.8 ± 0.2	16.3 ± 0.2	0.164	12.0

hexagonal character (h) and the other with cubic character (k), with the population ratio of 1:1. In 6H-SiC, there are three types of silicon sites, one with a hexagonal character (h) and the other two with a cubic character (k_1, k_2), with the population ratio of 1:1:1. Now, we assign the V_{Si}^-(I) and the V_{Si}^-(II) spectra to these inequivalent silicon sites. In both 4H-SiC and 6H-SiC, the difference in the principal values between $\mathbf{A}^{13}$C(C1) and $\mathbf{A}^{13}$C(C2) is smaller in V_{Si}^-(II) than in V_{Si}^-(I). The polar angle θ of the unique axis of $\mathbf{A}^{13}$C(C2) is closer to tetrahedral angle (109.47°) in V_{Si}^-(II)(109.2° in 4H-SiC and 109.1° in 6H-SiC) than in V_{Si}^-(I) (110.0° in 4H-SiC and 110.0° in 6H-SiC). Thus, the deviation from an ideal tetrahedron is smaller in V_{Si}^-(II) than in V_{Si}^-(I). It is likely that the vacancy at the hexagonal silicon site should be more distorted than the vacancy at the quasicubic silicon site. As seen from Figs. 2–4, the concentration ratio $[V_{Si}^-(\text{II})]/[V_{Si}^-(\text{I})]$ in 4H-SiC obtained from the intensity ratio between the corresponding ^{13}C hyperfine lines ($d_{\text{II}}/d_{\text{I}}$, $e_{\text{II}}/e_{\text{I}}$, $f_{\text{II}}/f_{\text{I}}$, $g_{\text{II}}/g_{\text{I}}$, and $j_{\text{II}}/j_{\text{I}}$) is ~1.4. The concentration ratio $[V_{Si}^-(\text{II})]/[V_{Si}^-(\text{I})]$ in 6H-SiC obtained from the intensity ratio between the corresponding ^{13}C hyperfine lines of the basal carbon atoms ($d_{\text{II}}/d_{\text{I}}$ in the case of the c axis spectrum shown in Fig. 7) is ~3.0. Since the deviation from an ideal tetrahedron of V_{Si}^-(I) is larger than that of V_{Si}^-(II), and since the concentration ratio $[V_{Si}^-(\text{II})]/[V_{Si}^-(\text{I})]$ in 6H-SiC is nearly twice as large as that in 4H-SiC, we assume that V_{Si}^-(I) and V_{Si}^-(II) are vacancies at the hexagonal silicon site and at quasicubic site(s), respectively. In the case that the EPR spectra of impurities at all three different sites of 6H-SiC are resolved, the difference of the EPR parameters between the hexagonal and quasicubic sites is much larger than that between two quasicubic sites.[9,16–24] In our case of V_{Si}^- in 6H-SiC, the difference of the EPR parameters between the two quasicubic sites was too small to be resolved by cw EPR method.

In Table II, $\mathbf{A}^{13}$C of V_{Si}^- in 3C-SiC[5] and $\mathbf{A}^{13}$C(C1) and $\mathbf{A}^{13}$C(C2) of T_{V2a} in 4H-SiC (Ref. 13) are included. The ^{13}C hyperfine matrix of the basal carbon atoms $\mathbf{A}^{13}$C(C2) of V_{Si}^-(II) in 4H- and 6H-SiC is closer to that of V_{Si}^- in 3C-SiC than that of V_{Si}^-(I) in 4H- and 6H-SiC. This fact supports the assignment that V_{Si}^-(I) is at hexagonal silicon site and V_{Si}^-(II) is at quasicubic site(s). The ^{13}C hyperfine matrices of

the axial carbon atoms $\mathbf{A}^{13}$C(C1) are similar among V_{Si}^- in 3C-SiC, V_{Si}^-(I, II) in 4H- SiC, V_{Si}^-(I, II) in 6H-SiC, and T_{V2a} in 4H-SiC. From the similarity of $\mathbf{A}^{13}$C(C1) and $\mathbf{A}^{13}$C(C2) between T_{V2a} and V_{Si}^-(I, II), the arrangement of four carbon atoms around the vacancy in T_{V2a} is similar to that of the isolated negatively charged vacancy V_{Si}^-(I,II). Thus, the small ZFS of T_{V2a} is ascribed to additional symmetry-lowering crystal field caused by possible presence of an accompanying nonparamagnetic impurity or defect located at some distance along [0001].[13]

From the ^{13}C hyperfine interaction of the NN carbon atoms, the symmetries of V_{Si}^-(I) and V_{Si}^-(II) both in 4H-SiC and in 6H-SiC are determined to be C_{3v}. Under T_d symmetry, the high spin ground state $^4A_2$ ($S=3/2$) arises from electronic configuration $a_1^2 t_2^3$. Under the C_{3v} symmetry, the t_2 triplet splits into a_1' and a doublet e. The high spin ground state $^4A_2$ ($S=3/2$) which is an orbitally non-degenerated state free from Jahn-Teller distortion is derived from the configurations $(a_1')e^2$ and $e^2(a_1')$.[13,32] So far, the single vacancies which have $S=3/2$ ground state are limited to those having T_d symmetry except T_{V2a} in 4H-SiC.[13] The lowering of the crystal field in T_{V2a} was ascribed to the possible presence of an impurity or defect at some distance along [0001]. In our present work, it is revealed that isolated vacancy V_{Si}^- in the hexagonal lattices of 4H-SiC and 6H-SiC does have $S=3/2$ ground state although with C_{3v} symmetry. Thus, threefold degenerate t_2 state under tetrahedral symmetry is not necessarily required to attain the high spin configuration of $S=3/2$. Our example in which three parallel spins are occupied in a_1' and e under C_{3v} symmetry demonstrates the important role of electron-electron interaction in determining the electronic state of vacancies of wide-gap semiconductor crystals such as SiC.

The intensity ratio of the ^{13}C hyperfine line relative to the primary line listed in Table I is slightly smaller than that is calculated from the natural abundance of ^{13}C. In V_{Si}^-(I, II) in 4H-SiC, the ratio $[V_{Si}^-(\text{II})]/[V_{Si}^-(\text{I})]$ obtained from the ^{13}C hyperfine lines of the axial carbon atoms is slightly smaller than that obtained from the ^{13}C hyperfine lines of the basal carbon atoms. The concentration ratio $[V_{Si}^-(\text{II})]/[V_{Si}^-(\text{I})]$ was obtained as the average among the peak hight ratios at several orientations. For the axial carbon atoms of V_{Si}^-(I, II) in 4H-SiC, the number of orientations where the ^{13}C hyperfine lines of V_{Si}^-(I) and V_{Si}^-(II) were resolved is limited. Since the signals from non-identified centers interfered with the weak ^{13}C hyperfine lines at several orientations and moreover the splitting of the line positions between V_{Si}^-(I) and V_{Si}^-(II) is small, measuring the ^{13}C hyperfine lines accurately was not easy. The fact that the ratio $[V_{Si}^-(\text{II})]/[V_{Si}^-(\text{I})]$ obtained from the ^{13}C hyperfine lines of the basal carbon atoms in 4H-SiC (1.4) is larger than that is calculated from the population ratio of silicon atoms between hexagonal and cubic sites (1.0) might suggest the difference in thermal stability between V_{Si}^-(I) and V_{Si}^-(II).

Even if the ZFS is vanishing, the high spin state might be detected by the splitting of hyperfine lines in the cw EPR measurements. From the second order perturbation treatment, the line position B of the $|S,M_S-1,m_I\rangle \Leftrightarrow |S,M_S,m_I\rangle$ transition is given as[33]

$$g\beta_e B = h\nu + Km_I + \frac{1}{2h\nu}\left\{|A_1|^2 m_I^2 + A_2 m_I (2M_S - 1)\right.$$

$$\left. + \frac{1}{2}A_3[I(I+1) - m_I^2]\right\}. \tag{3}$$

Details of the coefficients in Eq. (3) are given in the Appendix. In the case of $S = 3/2$, it is expected that the hyperfine line should split into three lines. However, in our case, the maximum magnitude of the splitting is estimated to be 0.005 mT which is smaller than the linewidth (0.022 mT in $4H$-SiC and 0.030 mT in $6H$-SiC).

IV. SUMMARY

The angular dependence of the ^{13}C hyperfine lines of the isolated negatively charged vacancy (V_{Si}^-) in electron-irradiated $4H$-SiC and $6H$-SiC has been measured by the X-band cw EPR method. In both $4H$-SiC and $6H$-SiC, two kinds of V_{Si}^-, denoted V_{Si}^-(I) and V_{Si}^-(II), respectively, have been distinguished. The C_{3v} symmetry with the arrangement of the four nearest-neighbor carbon atoms slightly distorted from a regular tetrahedron has been revealed in both V_{Si}^-(I) and V_{Si}^-(II).

From the difference in the degree of distortion from an ideal regular tetrahedron between V_{Si}^-(I) and V_{Si}^-(II) and from the difference in the concentration ratio $[V_{Si}^-(II)]/[V_{Si}^-(I)]$ between $4H$-SiC and $6H$-SiC, V_{Si}^-(I) and V_{Si}^-(II) are assigned to be arising from hexagonal site (h) and quasicubic site(s) (k in $4H$-SiC, k_1 and k_2 in $6H$-SiC), respectively. By revealing the C_{3v} symmetry of the isolated vacancy with $S = 3/2$, the important role of electron-electron interaction to attain the high spin configuration is demonstrated.

APPENDIX

The coefficients in Eq. (3) are given as follows:[33]

$$|A_1|^2 = (\tilde{\mathbf{k}} \cdot \mathbf{A} \cdot \tilde{\mathbf{A}} \cdot \mathbf{k}) - K^2, \tag{A1}$$

$$A_2 = \det \mathbf{A}/K, \tag{A2}$$

$$A_3 = \mathrm{Tr}\,\tilde{\mathbf{A}} \cdot \mathbf{A} - (\tilde{\mathbf{k}} \cdot \mathbf{A} \cdot \tilde{\mathbf{A}} \cdot \mathbf{k}), \tag{A3}$$

$$\mathbf{k} = \mathbf{A} \cdot \mathbf{g} \cdot \mathbf{h}/gK, \tag{A4}$$

$$K^2 = \tilde{\mathbf{h}} \cdot \tilde{\mathbf{g}} \cdot \tilde{\mathbf{A}} \cdot \mathbf{A} \cdot \mathbf{g} \cdot \mathbf{h}/g^2, \tag{A5}$$

$$g^2 = \tilde{\mathbf{h}} \cdot \tilde{\mathbf{g}} \cdot \mathbf{g} \cdot \mathbf{h}. \tag{A6}$$

The symbols $\mathbf{A}$, $\mathbf{g}$, and $\mathbf{h}$ represent the hyperfine matrix, the g matrix, and the unit vector that is parallel to the static field $\mathbf{B}$, respectively. The $\det \mathbf{A}$ in Eq. (A2) and the $\mathrm{Tr}\,\mathbf{A}$ in Eq. (A3) indicate the determinant of $\mathbf{A}$ and the trace of $\mathbf{A}$, respectively.

---

*To whom correspondence should be addressed.

[1] G.D. Watkins, in *Radiation Damage in Semiconductors*, edited by P. Baruch (Dunod, Paris, 1965), pp. 97–113.

[2] E.G. Sieverts, M. Sprenger, and C.A.J. Ammerlaan, Phys. Rev. B **41**, 8630 (1990).

[3] J. Isoya, H. Kanda, Y. Uchida, S.C. Lawson, S. Yamasaki, H. Itoh, and Y. Morita, Phys. Rev. B **45**, 1436 (1992).

[4] C.A. Coulson and M.J. Kearsley, Proc. R. Soc. London, Ser. A **241**, 433 (1957).

[5] H. Itoh, M. Yoshikawa, I. Nashiyama, S. Misawa, H. Okumura, and S. Yoshida, IEEE Trans. Nucl. Sci. **37**, 1732 (1990); H. Itoh, A. Kawasuso, T. Ohshima, M. Yoshikawa, I. Nashiyama, S. Tanigawa, S. Misawa, H. Okumura, and S. Yoshida, Phys. Status Solidi A **162**, 173 (1997).

[6] T.A. Kennedy and N.D. Wilsey, Phys. Rev. B **23**, 6585 (1981); T.A. Kennedy, N.D. Wilsey, J.J. Krebs, and G.H. Stauss, Phys. Rev. Lett. **50**, 1281 (1983).

[7] J. Hage, J.R. Niklas, and J.-M. Spaeth, Mater. Sci. Forum **10-12**, 259 (1986).

[8] T. Wimbauer, B.K. Meyer, A. Hofstaetter, A. Scharmann, and H. Overhof, Phys. Rev. B **56**, 7384 (1997).

[9] J. Schneider and K. Maier, Physica B **185**, 199 (1993).

[10] Among the terms which induce the zero-field splitting (ZFS), S^4 terms are not allowed in the spin Hamiltonian of $S = 3/2$. Since each term must be invariant under the point symmetry opera-tions, there are no S^2 terms for cubic symmetry. Thus, ZFS vanishes for $S = 3/2$ in the tetrahedral symmetry, see *The Physical Principles of Electron Paramagnetic Resonance* (Ref. 11)

[11] G.E. Pake and T.L. Estle, *The Physical Principles of Electron Paramagnetic Resonance*, 2nd ed. (Benjamin, New York, 1973).

[12] A. Zywietz, J. Furthmüller, and F. Bechstedt, Phys. Rev. B **59**, 15166 (1999).

[13] N. Mizuochi, S. Yamasaki, H. Takizawa, N. Morishita, T. Ohshima, H. Itoh, and J. Isoya, Phys. Rev. B **66**, 235202 (2002).

[14] A.H. Gomes de Mesquita, Acta Crystallogr. **23**, 610 (1967).

[15] A. Bauer, J. Kräußlich, L. Dressler, P. Kuschnerus, J. Wolf, K. Goetz, P. Käckell, J. Furthmüller, and F. Bechstedt, Phys. Rev. B **57**, 2647 (1998).

[16] H.H. Woodbury and G.W. Ludwig, Phys. Rev. **124**, 1083 (1961).

[17] A.G. Zubatov, I.M. Zaritskii, S.N. Lukin, E.N. Mokhov, and V.G. Stepanov, Fiz. Tverd. Tela (Leningrad) **27**, 322 (1985) [Sov. Phys. Solid State **27**, 197 (1985)].

[18] T. Matsumoto, O.G. Poluektov, J. Schmidt, E.N. Mokhov, and P.G. Baranov, Phys. Rev. B **55**, 2219 (1997).

[19] A.v. Duijn-Arnold, T. Ikoma, O.G. Poluektov, P.G. Baranov, E.N. Mokhov, and J. Schmidt, Phys. Rev. B **57**, 1607 (1998).

[20] E.N. Kalabukhova, N.N. Kabdin, and S.N. Lukin, Fiz. Tverd. Tela (Leningrad) **29**, 2532 (1987) [Sov. Phys. Solid State **29**, 1461 (1987)].

[21] A.v. Duijn-Arnold, R. Zondervan, J. Schmidt, P.G. Baranov, and

E.N. Mokhov, Phys. Rev. B **64**, 085206 (2001).

[22] A.I. Veinger, A.G. Zabrodskii, G.A. Lomakina, and E.N. Mokhov, Fiz. Tverd. Tela (Leningrad) **28**, 1659 (1986) [Sov. Phys. Solid State **28**, 917 (1986)].

[23] P.G. Baranov, I.V. Ilyin, E.N. Mokhov, H.J. von Bardeleben, and J.L. Cantin, Phys. Rev. B **66**, 165206 (2002).

[24] J. Baur, M. Kunzer, and J. Schneider, Phys. Status Solidi A **162**, 153 (1997).

[25] P.G. Baranov, E.N. Mokhov, S.B. Orlinski, and J. Schmidt, Physica B **308-310**, 680 (2001); S.B. Orlinski, J. Schmidt, E.N. Mokhov, and P.G. Baranov, Phys. Rev. B **67**, 125207 (2003).

[26] B.G. Segal, M. Kaplan, and G.K. Fraenkel, J. Chem. Phys. **43**, 4191 (1965).

[27] R.D. Allendoerfer, J. Chem. Phys. **55**, 3615 (1971).

[28] T. Chang, D. Foster, and A.H. Kahn, J. Res. Natl. Bur. Stand. **83**, 133 (1978).

[29] G. Audi and A.H. Wapstra, Nucl. Phys. A **565**, 1 (1993).

[30] J.A. Weil, J.R. Bolton, and J.E. Wertz, *Electron Paramagnetic Resonance* (Wiley, New York, 1994).

[31] J.R. Morton and K.F. Preston, J. Magn. Reson. (1969-1992) **30**, 577 (1978).

[32] F.A. Cotton, *Chemical Applications of Group Theory*, 2nd ed. (Wiley, New York, 1971).

[33] M. Iwasaki, J. Magn. Reson. (1969-1992) **16**, 417 (1974).